Supporting information for "Polarization-bound quasi-continuum states are responsible for the 'blue tail' in the optical absorption spectrum of the aqueous electron"

Leif D. Jacobson and John M. Herbert*

This document provides additional details regarding the TD-DFT calculations and the calculations utilizing the one-electron model. In addition, a complete citation for Ref. 3 in the paper is provided in Ref. 1 below.

1 TD-DFT calculations

1.1 Functional and basis set

TD-DFT calculations employ a long-range-corrected (LRC) version of the "BOP" density functional, where BOP indicates the combination of the Becke exchange (B88) functional[2] with the "one-parameter progressive" (OP) correlation functional.[3] A short-range version of the B88 functional (μB88) was constructed according to the procedure described in Ref. 4, and the total exchange–correlation functional is

$$E_{xc}^{\text{LRC-}\mu\text{BOP}} = E_c^{\text{OP}} + E_x^{\mu\text{B88,SR}} + E_x^{\text{HF,LR}} \ , \tag{S1}$$

where "SR" and "LR" indicate that only the short-range or long-range parts of the Coulomb operator are used to evaluate certain energy components. Our group has implemented this and other LRC functionals[5–7] within the Q-Chem electronic structure program.[8] Within Q-Chem, the functional denoted in Eq. (S1) is known as LRC-μBOP, although the value of the Coulomb attenuation parameter, μ, must be set by the user.

*herbert@chemistry.ohio-state.edu

The LRC-μBOP functional with $\mu = 0.33\ a_0^{-1}$ has been shown to afford vertical electron binding energies (VEBEs) for $(H_2O)_n^-$ clusters that are comparable to those obtained at the CCSD(T) level.[9,10] In addition, we have shown[6,11] that LRC functionals with comparable values of μ remove the spurious, low-energy charge-transfer excited states that would otherwise be encountered in calculations such as these.[12] Inadvertently, we used a slightly different value for the Coulomb attenuation parameter, $\mu = 0.37\ a_0^{-1}$, for the TD-DFT calculations reported in this work, as opposed to the value $\mu = 0.33\ a_0^{-1}$ that was used in previous VEBE benchmarks. However, a comparison of TD-DFT excitation energies for these two values of μ, at a small number of randomly-chosen solvent configurations, reveals that the excitation energies differ on average by only 0.06 eV, and in no case by more than 0.09 eV.

As in earlier QM/MM calculations of bulk e^-(aq), carried out at the CIS level by Skrob *et al.*,[13] we use the 6-31+G* basis set for these calculations. Our own prior work on $(H_2O)_n^-$ clusters[14–16] has shown that somewhat more diffuse basis sets are necessary to describe weakly-bound isomers, but VEBEs for cavity-like isomers converge much more quickly as a function of the number of diffuse basis functions. Since the energy of the neutral cluster changes very little as additional diffuse shells are added, we regard convergence of the VEBE as evidence that the description of the singly-occupied MO (SOMO) has converged. It is worth noting that the most diffuse Gaussian basis function in the 6-31+G* basis set has a full width at half maximum of 4.6 Å, which is large compared to the distance between nearest-neighbor water molecules. The SG-1 quadrature grid[17] is used in all calculations, which has been shown to be adequate even in the presence of highly diffuse basis functions.[14] All TD-DFT calculations were performed using Q-Chem.[8]

As one marches up the manifold of states in the TD-DFT calculation, one expects that these states will become increasingly sensitive to the diffuseness of the basis set. Therefore as a check, we also computed the absorption spectrum using the same functional but a much more diffuse basis set, 6-31(1+,2+)G*, which includes two additional sets of diffuse s functions on the hydrogen atoms. (Details of the simulation procedure used to obtain the spectra are discussed in Section 1.2 of this document.) Figure S1 shows that the results are quite similar to those obtained with the more compact 6-31+G* basis. In particular, the peak absorption intensity and the width of the Gaussian feature are reproduced essentially quantitatively, while a non-trivial tail is observed at higher excitation energies. This blue tail is

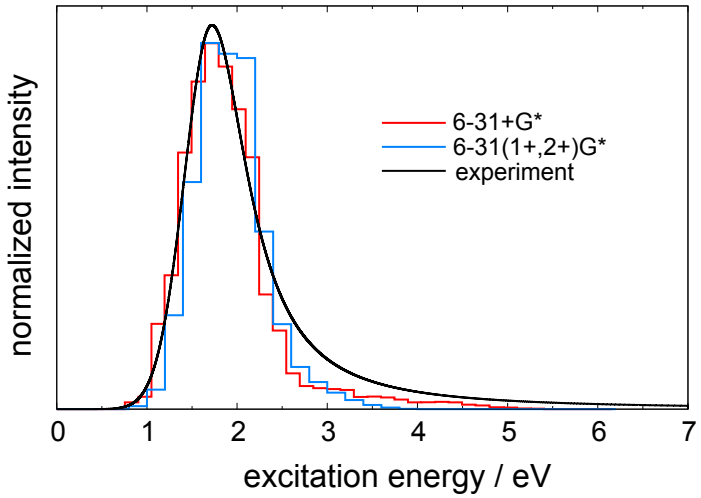

Figure S1: Comparison of simulated TD-DFT absorption spectra, computed with the LRC-μBOP functional using two different basis sets.

somewhat attenuated in the more diffuse basis set, because this basis lowers the energies of the higher-lying states to a much greater extent that for the first few excited states. To obtain significant intensity above ~ 3.5 eV in the larger basis, we would need to compute a much larger number of excited states, which would make the calculations prohibitively expensive. For this reason, and because we are somewhat wary of having basis functions that extend well into the MM region, we report the 6-31+G* calculations in Fig. 1 of the manuscript.

1.2 Simulation procedure

Geometries for the TD-DFT calculations were obtained from a simulation of an excess electron in bulk liquid water. This simulation employed the one-electron pseudopotential model developed by Turi and Borgis,[18] a model that we selected because it has been used extensively in recent hydrated-electron simulations,[18–25] and because it provides a more accurate value for the e^-(aq) absorption maximum than any other non-polarizable one-electron model. (Our polarizable model is more accurate in this respect, but we used

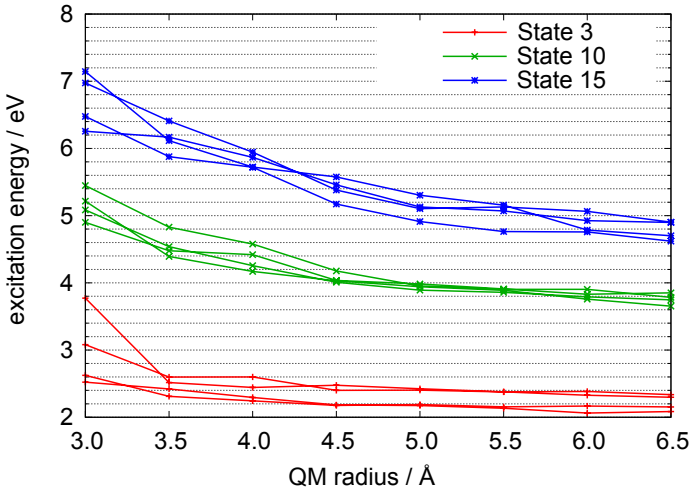

Figure S2: Convergence of the TD-DFT [LRC-μBOP/6-31+G*] excitation energies as a function of the radius of the QM region, for three different randomly-selected snapshots taken from a bulk e^-(aq) simulation.

the Turi–Borgis model for these calculations because we wanted the TD-DFT calculations to be completely independent of the calculations performed using our own one-electron model, in order to report results from two completely independent computational paradigms.)

Four independent, equilibrated trajectories were propagated at $T = 298$ K, using a simulation code that we have described previously.[10] These simulations were performed in a periodic unit cell, 18.1671 Å on a side, and snapshots were extracted every 0.5 ps. All H_2O molecules having an O or H atom within 5.5 Å of the centroid of the electron's wavefunction were described using DFT (corresponding to an average of 28 water molecules in the QM region), whereas remaining water molecules (out to a distance of 50 Å from the centroid of the wavefunction, or $\sim 18,000$ water molecules) were described using point charges ($q_O = -0.82, q_H = +0.41$). The 5.5 Å radius for the QM region was chosen based upon convergence tests (see Fig. S2) for a small number of snapshots, which reveal that the first ten excitation energies are converged at this size, and the next five states are nearly converged (to within $\sim$0.1–0.2 eV).

In all, 124 snapshots were used to construct the histogram that appears

in Fig. 1 of the paper. The overall shape of this histogram is unchanged if the number of snapshots is reduced by a factor of two, although somewhat larger bin widths are then required to obtain a smooth spectrum. We take this as an indication that the spectrum is converged with respect to statistical sampling of liquid configurations.

2 One-electron model

Our one-electron model is based upon a polarizable electron–water pseudopotential that we have recently developed. For details regarding the construction of this model and its performance relative to various experimental and *ab initio* benchmarks, the reader is referred to Ref. 26. Previously, we had developed an alternative pseudopotential for $(H_2O)_n^-$ calculations,[10] but subsequent analysis, as documented in Ref. 26, demonstrated that this potential is inappropriate for simulation of e^-(aq) in bulk water.

In Ref. 26, we also discuss the convergence of the bulk e^-(aq) calculations with respect to the simulation cell size, which is an important issue for these excited-state calculations. Based upon these tests, the calculations described in this work utilize a cubic simulation cell of length 26.2015 Å that contains 600 water molecules, corresponding to a water density of 0.997 g/cm^3, at $T =$ 298 K. This cell size is more than sufficient to converge structural properties and low-lying excitation energies. (The radii of gyration of the p states are essentially independent of simulation cell size, for example.[26]) The higher excited states ($\sim$3 eV and above) are probably not (quite) converged, even in this very large box, hence we list their radii of gyration as simply "$>$ 10 Å", since this value would increase somewhat in a larger simulation cell. A larger simulation cell would likely red-shift the "higher bound states" in Fig. 2(b) of the paper, thus improving the agreement with the experimental line shape. Because the mixed quantum/classical dynamics is rather expensive in these larger cells, we have not done this calculation.

Absorption spectra are computed using several independent, ground-state trajectories for e^-(aq) in the aforementioned periodic box. Each simulation is $\approx$ 21 ps in length, and is propagated with a time step of 1 fs using flexible water molecules and full Ewald summation (as described in Ref. 26) for the long-range electrostatics, and a Nosé-Hoover thermostat chain to simulate the NVT ensemble. The wavefunction is represented on a cubic grid with $\Delta x \approx 0.93$ eV. (Excitation energies appear to be converged with respect to

Δx.) These simulations were performed with a home-built simulation code that we have described previously.[10] Following the ground-state trajectory calculations, we calculate the lowest 29 excitation energies from each of $\sim$ 1000 snapshots, and bin these to form an absorption spectrum.

References

[1] Garrett, B. C.; Dixon, D. A.; Camaioni, D. M.; Chipman, D. M.; Johnson, M. A.; Jonah, C. D.; Kimmel, G. A.; Miller, J. H.; Rescigno, T. N.; Rossky, P. J.; Xantheas, S. S.; Colson, S. D.; Laufer, A. H.; Ray, D.; Barbara, P. F.; Bartels, D. M.; Becker, K. H.; Bowen, Jr., K. H.; Bradforth, S. E.; Carmichael, I.; Coe, J. V.; Corrales, L. R.; Cowin, J. P.; Dupuis, M.; Eisenthal, K. B.; Franz, J. A.; Gutowski, M. S.; Jordan, K. D.; Kay, B. D.; LaVerne, J. A.; Lymar, S. V.; Madey, T. E.; McCurdy, C. W.; Meisel, D.; Mukamel, S.; Nilsson, A. R.; Orlando, T. M.; Petrik, N. G.; Pimblott, S. M.; Rustad, J. R.; Schenter, G. K.; Singer, S. J.; Tokmakoff, A.; Wang, L.-S.; Wittig, C.; Zwier, T. S. *Chem. Rev.* **2005**, *105*, 355.

[2] Becke, A. D. *Phys. Rev. A* **1988**, *38*, 3098.

[3] Tsuneda, T.; Suzumura, T.; Hirao, K. *J. Chem. Phys.* **1999**, *110*, 10664.

[4] Iikura, H.; Tsuneda, T.; Yanai, T.; Hirao, K. *J. Chem. Phys.* **2001**, *115*, 3540.

[5] Rohrdanz, M. A; Herbert, J. M. *J. Chem. Phys.* **2008**, *129*, 034107.

[6] Lange, A. W.; Rohrdanz, M. A.; Herbert, J. M. *J. Phys. Chem. B* **2008**, *112*, 6304.

[7] Rohrdanz, M. A.; Martins, K. M.; Herbert, J. M. *J. Chem. Phys.* **2009**, *130*, 054112.

[8] Shao, Y.; Fusti-Molnar, L.; Jung, Y.; Kussmann, J.; Ochsenfeld, C.; Brown, S. T.; Gilbert, A. T. B.; Slipchenko, L. V.; Levchenko, S. V.; O'Neill, D. P.; Jr., R. A. D.; Lochan, R. C.; Wang, T.; Beran, G. J. O.; Besley, N. A.; Herbert, J. M.; Lin, C. Y.; Van Voorhis, T.; Chien, S. H.; Sodt, A.; Steele, R. P.; Rassolov, V. A.; Maslen, P. E.; Korambath,

P. P.; Adamson, R. D.; Austin, B.; Baker, J.; Byrd, E. F. C.; Dachsel, H.; Doerksen, R. J.; Dreuw, A.; Dunietz, B. D.; Dutoi, A. D.; Furlani, T. R.; Gwaltney, S. R.; Heyden, A.; Hirata, S.; Hsu, C.-P.; Kedziora, G.; Khalliulin, R. Z.; Klunzinger, P.; Lee, A. M.; Lee, M. S.; Liang, W.; Lotan, I.; Nair, N.; Peters, B.; Proynov, E. I.; Pieniazek, P. A.; Rhee, Y. M.; Ritchie, J.; Rosta, E.; Sherrill, C. D.; Simmonett, A. C.; Subotnik, J. E.; Woodcock III, H. L.; Zhang, W.; Bell, A. T.; Chakraborty, A. K.; Chipman, D. M.; Keil, F. J.; Warshel, A.; Hehre, W. J.; Schaefer III, H. F.; Kong, J.; Krylov, A. I.; Gill, P. M. W.; Head-Gordon, M. *Phys. Chem. Chem. Phys.* **2006**, *8*, 3172.

[9] Yagi, K.; Okano, Y.; Sato, T.; Kawashima, Y.; Tsuneda, T.; Hirao, K. *J. Phys. Chem. A* **2008**, *112*, 9845.

[10] Jacobson, L. D.; Williams, C. F.; Herbert, J. M. *J. Chem. Phys.* **2009**, *130*, 124115.

[11] Lange, A. W.; Herbert, J. M. *J. Am. Chem. Soc.* **2009**, *131*, 3913.

[12] Lange, A.; Herbert, J. M. *J. Chem. Theory Comput.* **2007**, *3*, 1680-.

[13] Shkrob, I. A.; Glover, W. J.; Larsen, R. E.; Schwartz, B. J. *J. Phys. Chem. A* **2007**, *111*, 5232.

[14] Herbert, J. M.; Head-Gordon, M. *J. Phys. Chem. A* **2005**, *109*, 5217.

[15] Herbert, J. M.; Head-Gordon, M. *Phys. Chem. Chem. Phys.* **2006**, *8*, 68.

[16] Williams, C. F.; Herbert, J. M. *J. Phys. Chem. A* **2008**, *112*, 6171.

[17] Gill, P. M. W.; Johnson, B. G.; Pople, J. A. *Chem. Phys. Lett.* **1993**, *209*, 506.

[18] Turi, L.; Borgis, D. *J. Chem. Phys.* **2002**, *117*, 6186.

[19] Turi, L.; Sheu, W.-S.; Rossky, P. J. *Science* **2005**, *309*, 914.

[20] Turi, L.; Madarász, Á.; Rossky, P. J. *J. Chem. Phys.* **2006**, *125*, 014308.

[21] Borgis, D.; Rossky, P. J.; Turi, L. *J. Chem. Phys.* **2006**, *125*, 064501.

[22] Borgis, D.; Rossky, P. J.; Turi, L. *J. Chem. Phys.* **2007**, *127*, 174508.

[23] Madarász, Á.; Rossky, P. J.; Turi, L. *J. Chem. Phys.* **2007**, *126*, 234707.

[24] Madarasz, A.; Rossky, P. J.; Turi, L. *J. Chem. Phys.* **2009**, *130*, 124319.

[25] Tay, K. A.; Boutin, A. *J. Phys. Chem. B* **2009**, *113*, 11943.

[26] Jacobson, L. D.; Herbert, J. M. *J. Chem. Phys.* (submitted).